J. Fluid Mech. (1978), *vol.* 84, *part* 4, *pp.* 705–715
Printed in Great Britain

Measurements of velocity distributions in the laminar wake of a flat plate

By MICHIO NISHIOKA AND TOSIO MIYAGI
College of Engineering, University of Osaka Prefecture, Japan

(Received 12 April 1977)

The two-dimensional wake of a thin flat plate parallel to the stream was maintained laminar and steady at Reynolds numbers up to 3000 in a low-turbulence wind tunnel. Velocity distributions in the wake were measured in detail for Reynolds numbers from 20 to 3000. One of the interesting results is the appearance of a velocity overshoot, namely that the velocity in the outer part of the shear layer exceeds that of the uniform flow in the vicinity of the trailing edge. Comparisons between the experimental results and Goldstein's theoretical predictions show good agreement in the far wake irrespective of the Reynolds number, but not in the near wake even at higher Reynolds numbers, in particular immediately behind the trailing edge.

1. Introduction

Laminar, steady, two-dimensional flow past a finite flat plate aligned parallel to a uniform stream is one of the most fundamental problems in fluid mechanics. It is of theoretical and experimental interest to investigate how the wake of the plate is formed under the sudden change in boundary at the trailing edge. This problem was first treated theoretically by Goldstein (1930, 1933), who analysed the development of the velocity distribution in the wake using the boundary-layer approximation and further assuming the wake to be isobaric. Recently, in order to improve his result, various authors have attempted to solve the problem on the basis of the full Navier–Stokes equations of motion (Talke & Berger 1970; Schneider & Denny 1971; Stewartson 1974; and so on).

In an experiment, it is difficult to maintain a laminar wake without any growing disturbances at high Reynolds numbers, owing to the inherent instability of the wake. Hollingdale (1940) and Taneda (1956) observed that oscillation occurs in the wake beyond $R = 600 \sim 700$ (R being the Reynolds number based on the speed of the uniform stream U_∞ and the length of the plate l). Sato & Kuriki (1961) and Mattingly & Criminale (1972) also observed the wake to investigate the instability, and there were growing disturbances in their wakes. Before Hollingdale (1940), Fage & Falkner (cited in Goldstein 1933) measured velocity distributions in the wake at $R \doteqdot 10^5$, but the wake was turbulent just behind the trailing edge. So far as the completely laminar wake is concerned, it seems that no experimental data are available on the velocity field except those for $R = 409$ obtained by Hollingdale (1940) and those for $R = 200$–300 obtained by Grove, Petersen & Acrivos (1964). It may be said that up to the present the detailed wake structure in the completely laminar state has not been fully established by experiment.

	Dimensions of plate (mm)				Reynolds number R obtained	Streamwise region of wake survey, x/l
	Span	Length l	Thickness: Maximum	Thickness: Rear edge		
Plate I	200	2·0	0·03	0·03	20, 100	$-2 \sim 20$
Plate II	200	7·8	0·05	0·05	400	$0 \sim 20$
Plate III	200	70·0	1·0	0·1	1200, 3000	$0 \sim 1{\cdot}75$

TABLE 1. Dimensions of flat plate, Reynolds numbers obtained and streamwise region of wake survey.

Earlier, the first author made a wind-tunnel experiment on the steady wake of a circular cylinder at low Reynolds numbers (Nishioka & Sato 1974), therefore the same equipment and techniques could be used in the present investigation. We obtained a completely laminar wake for the flat plate up to $R = 3000$ in the same low-turbulence wind tunnel. The present paper contains results of hot-wire measurements of the velocity distribution in the laminar wake for $R = 20$, 100, 400, 1200 and 3000. In this paper, we intend to compare the solution given by Goldstein (1930, 1933) with our experimental results on the wake development, and to clarify its structure.

2. Experimental procedure

The experiment was conducted in a suction-type wind tunnel which has a test section 20 × 20 cm in cross-section and 60 cm in length. The tunnel provides a uniform flow with a velocity variation of less than 1 % over the region of wake survey and less then 2 % over the entire cross-section excluding the wall boundary layer. In the present experiment the velocity of the uniform flow ranged from 8 to 80 cm/s. The residual turbulence was 0·01 % at 20 cm/s with a low cut-off at 8 Hz. At 70 cm/s the level was the same with a low cut-off at 15 Hz. Velocity measurements were made with a constant-temperature hot-wire anemometer and a linearizer which were specially designed and constructed for measurements at wind speeds below 150 cm/s (Nishioka 1973). The hot wire was mounted on a three-dimensional traversing mechanism. Details of the tunnel, the calibration of the anemometer and problems associated with measurements at low wind speeds are described in the previous paper (Nishioka & Sato 1974).

A laminar, steady, two-dimensional wake was realized up to $R = 3000$. No velocity fluctuations grew in the wake even beyond $R = 3000$, by virtue of the fact that the residual turbulence was kept quite low as noted above. However, the critical Reynolds number for the onset of the instability was not examined, because it is outside the scope of the present investigation.

Systematic measurements of the velocity distribution across the wake were made at Reynolds numbers of 20, 100, 400, 1200 and 3000, which were obtained by using three kinds of flat plate, as shown in table 1. For plates I and II phosphor bronze ribbons were used, and their thickness was constant from the leading to the trailing edge. The ribbon spanned the test section vertically, under tension by means of weights. Plate III was made of aluminium sheeting 1 mm thick and was machined to

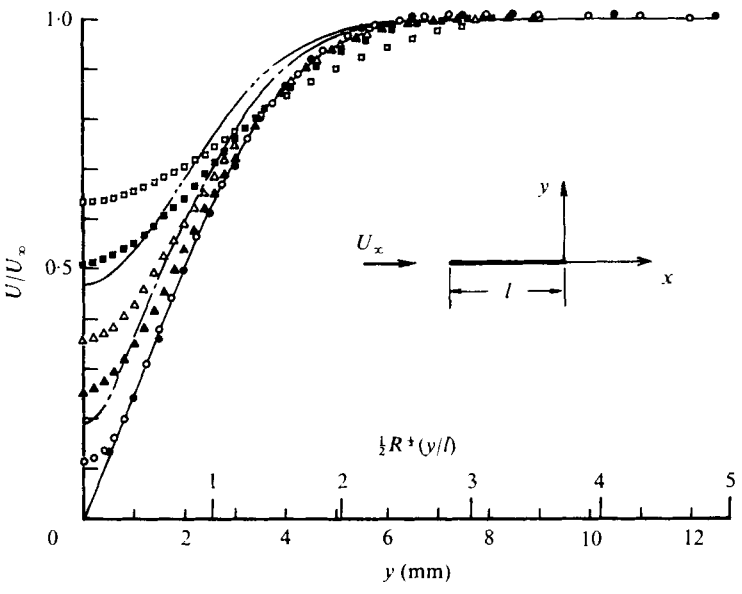

FIGURE 1. Velocity distributions in the near wake at $R = 3000$. Results of Goldstein's near-wake solution are compared with our measurements.

Goldstein:	——	— · —		— · · —		
x/l	0	0·0135		0·256		
Present:	●	○	▲	△	■	□
x/l	0	0·0285	0·15	0·30	0·70	1·5

have a round leading edge and a sharp trailing edge; the half-angle of the wedge-shaped trailing edge was about 1·5°. Alignment of the flat plate with the uniform flow was accomplished by confirming that the velocity distribution was symmetric just behind the trailing edge.

As previously discussed in Nishioka & Sato (1974), when a hot wire approaches a solid wall the rate of heat loss increases considerably owing to the direct heat conduction to the wall, and the anemometer indicates a larger apparent velocity. This wall effect can be appreciable when the wire is within 2 mm from the wall at zero wind speed, so we excluded all the data supposed to be contaminated by the wall effect in the present paper.

3. Results and discussion

At $R = 20$, 100, 400, 1200 and 3000, the velocity distributions were measured at various x/l stations in the region shown in table 1, x being the downstream distance from the trailing edge. In this paper, only part of the data are presented to concentrate our attention on the development of the wake.

3.1. *Velocity distribution across wake*

The initial development of the wake immediately behind the trailing edge in the case $R = 3000$ is shown in figure 1. Since the measured velocity field was confirmed to be symmetric with respect to the centre-line of the wake, only half is drawn for each

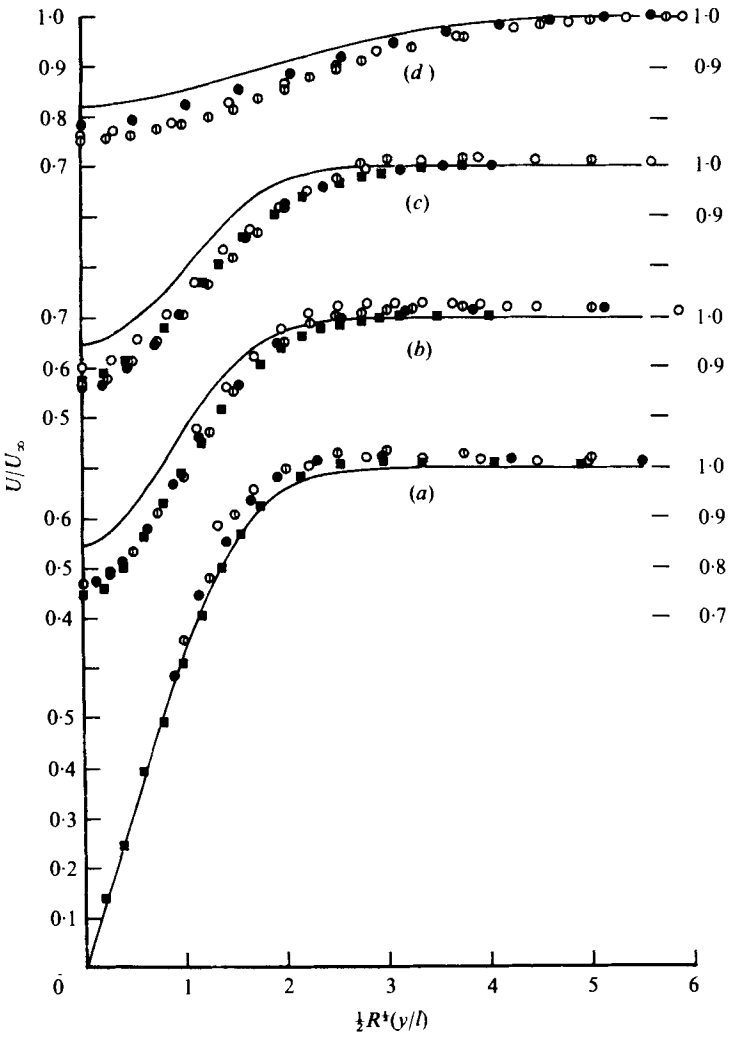

FIGURE 2. Wake development at R = 20, 100, 400, 3000. Results of Goldstein's far-wake solution are compared with our measurements.

		Present results				Goldstein
		○	◑	●	■	——
R		20	100	400	3000	Arbitrary
x/l	(a)	0	0	0	0	0
	(b)	0·5	0·5	0·54	0·50	0·50
	(c)	1·0	1·0	1·05	1·10	1·00
	(d)	5·0	5·0	5·15	—	5·00

distribution. For comparison, the theoretical results of Goldstein (1930) for the near wake are included in this figure. The distance y from the centre-line of the wake and the corresponding non-dimensional distance $\frac{1}{2}R^{\frac{1}{2}}(y/l)$ adopted by Goldstein are both given on the abscissa. Goldstein assumed the velocity distribution at the trailing edge to be of the Blasius type. The measured distribution at $x/l = 0$ agrees almost

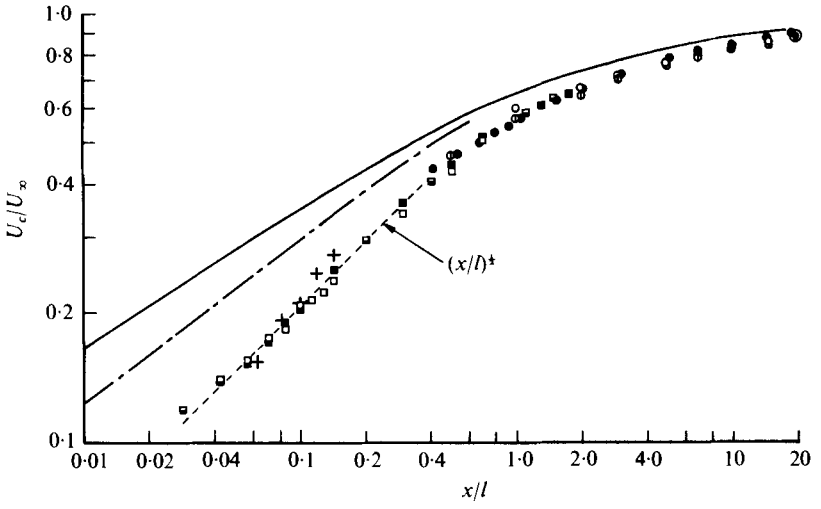

FIGURE 3. Non-dimensional centre-line velocity U_c/U_∞ *vs.* x/l in wakes at R = 20–3000. ——, theoretical result of Goldstein; — · —, theoretical result of Schneider & Denny. Our experimental points fall on the single curve $U_c/U_\infty \propto (x/l)^{\frac{1}{2}}$ for $x/l < 0{\cdot}3$, as shown by the broken line.

	Present results					Mattingly & Criminale
	○	⊙	●	□	■	+
R	20	100	400	1200	3000	$\doteqdot 10^4$

exactly with the Blasius profile, so that it appears that his assumption is valid at higher Reynolds numbers. In the subsequent development of the velocity distribution, however, there are distinct differences between the present data and his theoretical prediction. First, in the present experiment the velocity on the centre-line of the wake does not recover so rapidly as his theoretical prediction; this will be made clearer in figure 3. Second, in his prediction the velocity recovers in the outer part of the wake too, so that even at x/l = 0·0135 the distribution deviates essentially from the Blasius profile. However, deviation from the Blasius profile proceeds only in the portion around the centre-line of the wake; moreover, the outer part remains almost unchanged even up to x/l = 0·15 in the present wake.

Figure 2 also illustrates the wake development, comparing our velocity distributions for various different Reynolds numbers with each other at x/l = 0, 0·5, 1 and 5. Because of the wall effect mentioned above, the velocity data close to the plate are omitted here. We see that the distribution U/U_∞ *vs.* $\frac{1}{2}R^{\frac{1}{2}}(y/l)$ does not depend much on R in the far wake. Indeed, already at x/l = 1 the distributions for R = 20–3000 are brought close to each other by introducing this modified abscissa.

Another interesting feature demonstrated in figure 2 is the existence of the velocity overshoot in the outer part of the wake. At x/l = 0, its maximum value is 0·02 ~ 0·03 U_∞ for R = 20 ~ 400 and 0·01 U_∞ for R = 3000, decreasing as the Reynolds number increases. Afterwards, the overshoot becomes too small to be detected beyond x/l = 3, 2, 0·8 and 0·07 at R = 20, 100, 400 and 3000 respectively. It should be added here that in the cases R = 20–100 the overshoot appears even at x/l = −0·5. The overshoot would not appear in the case of a plate semi-infinite downstream.

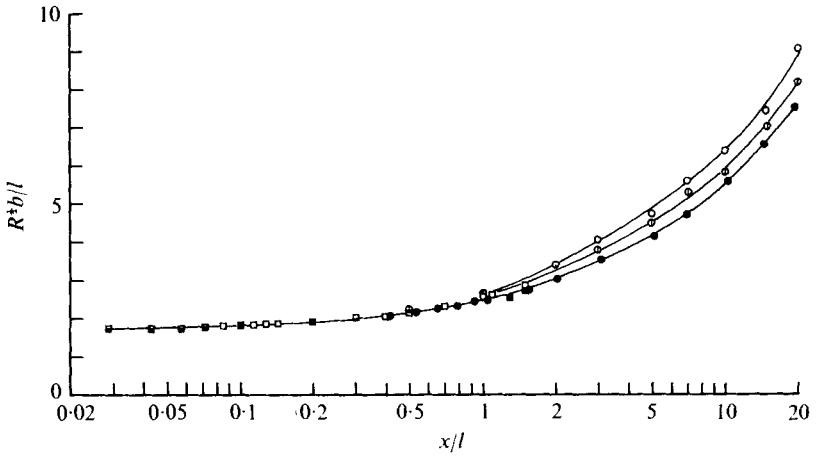

FIGURE 4. Non-dimensional half-width of wake $R^{\frac{1}{2}}b/l$ *vs.* x/l in wakes at R = 20–3000.

	○	⊙	●	□	■
R	20	100	400	1200	3000

Thus, in the present case, it may be said that the velocity overshoot is closely related to the sudden change in boundary at the trailing edge.

Comparisons are also made in figure 2 between our results and the theoretical distributions (the Blasius profile and Goldstein's (1933) results). At the trailing edge, our distributions lie considerably above the Blasius profile, in particular at lower Reynolds numbers. This feature and the existence of the velocity overshoot both clearly indicate that in the neighbourhood of the trailing edge the pressure is less than its ambient value. The comparisons with the results of Goldstein show that his solution for the far wake predicts well general features of the wake development. This has been already found by Hollingdale (1940), who compared velocity data for a wake at R = 409 with Goldstein's far-wake solution.

3.2. *Centre-line velocity and half-width of wake*

The non-dimensional centre-line velocity U_c/U_∞ is plotted against x/l in figure 3. Measurements by Mattingly & Criminale (1972) for $R \doteqdot 10^4$ are included together with ours. These experimental points for various Reynolds numbers fall on a single curve, suggesting that the relation between U_c/U_∞ and x/l does not depend much on R. The full line gives the solution of Goldstein (1930, 1933), which explains the observations well, in particular beyond $x/l = 1$. Close to the trailing edge, however, his solution indicates that $U_c/U_\infty \propto (x/l)^{\frac{1}{3}}$ for $x/l < 0{\cdot}1$, while in the present wakes at R = 1200 and 3000 we find $U_c/U_\infty \propto (x/l)^{\frac{1}{2}}$ for $x/l < 0{\cdot}3$, as shown by the broken line. Hence, in the initial development of the wake, there is a remarkable difference between these results, as already pointed out in figure 1. The dot–dash line is the result obtained by Schneider & Denny (1971) by applying second-order boundary-layer theory and will be mentioned in § 3.5.

In figure 4, the half-width of the wake b is plotted against x/l in the dimensionless form $R^{\frac{1}{2}}b/l$. It is seen that all the experimental points for R = 400, 1200 and 3000 around $x/l = 1$ fall on a single curve too, so that the relation $R^{\frac{1}{2}}b/l$ *vs.* x/l is also

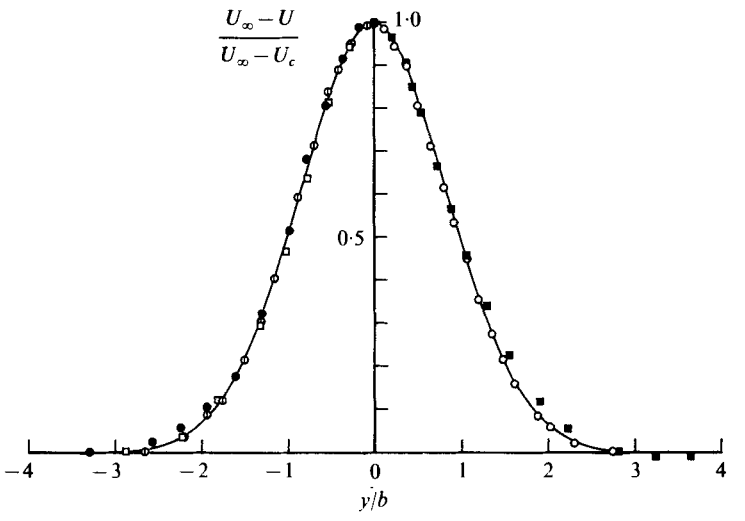

FIGURE 5. Velocity defect distributions in wakes at R = 20–3000. The Gaussian distribution (full line) is compared with our measurements.

	○	ⓘ	●	□	■
R	20	100	400	1200	3000
x/l	3	10	1·05	0·50	0·0285

almost independent of R at higher Reynolds numbers. But at lower Reynolds numbers this relation depends on R appreciably. At R = 20–400, the well-known relation $b/l \propto (x/l)^{\frac{1}{2}}$ seems to hold beyond x/l = 10.

3.3. *Velocity defect distribution*

For the velocity defect distribution in the wake, shown in figure 5, we may compare the following Gaussian distribution with the present measurements at various Reynolds numbers and x/l stations:

$$(U_\infty - U)/(U_\infty - U_c) = \exp\{-0{\cdot}693\,(y/b)^2\}.$$

We may suppose from this figure that the Gaussian distribution fits the actual distributions in the near as well as the far wake. Therefore, from the data for U_c/U_∞ and b/l given in figures 3 and 4 we can determine the wake velocity field except for the velocity overshoot.

3.4. *Displacement thickness, momentum thickness and drag coefficient*

From the measured velocity distributions, the displacement thickness δ^* and the momentum thickness θ, which are defined as

$$\delta^* = \frac{1}{U_m}\int_{-y_m}^{y_m}(U_m - U)\,dy, \quad \theta = \frac{1}{U_m^2}\int_{-y_m}^{y_m} U(U_m - U)\,dy,$$

were calculated, where y_m denotes the ordinate at which the velocity reaches its maximum value U_m. In figure 6, $R^{\frac{1}{2}}\delta^*/l$ and $R^{\frac{1}{2}}\theta/l$ are plotted against x/l. For comparison, the Blasius values $R^{\frac{1}{2}}\delta^*/l$ = 3·46 and $R^{\frac{1}{2}}\theta/l$ = 1·33 are denoted by

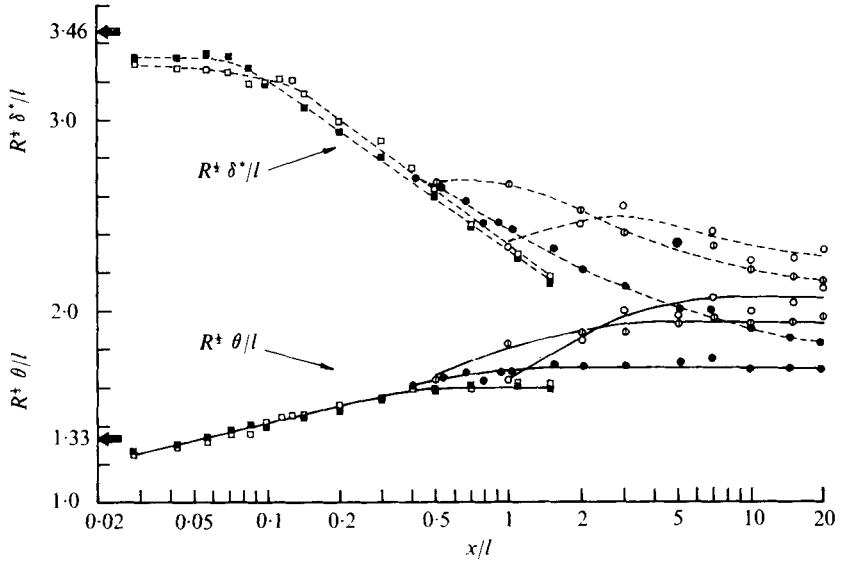

FIGURE 6. Streamwise variation of non-dimensional displacement thickness $R^{\frac{1}{2}}\delta^*/l$ and non-dimensional momentum thickness $R^{\frac{1}{2}}\theta/l$ at R = 20–3000.

R	○ 20	⊙ 100	● 400	□ 1200	■ 3000

Reynolds number, R ...	20	100	200	400	500	1000	1200	2000	3000
$R^{\frac{1}{2}}C_D$									
Dennis & Dunwoody	4·32	3·76	—	—	3·27	3·17	—	3·05	—
Dennis & Chang	4·51	3·74	3·48	—	—	—	—	—	—
Present	4·2	3·9	—	3·4	—	—	3·2	—	3·2

TABLE 2. Drag coefficient.

arrows on the ordinate. The momentum thickness, shown as the smoothed full lines, increases with x/l in the near wake, but eventually levels off far downstream, as might be expected. This constant value for each Reynolds number is related to the drag coefficient by

$$C_D = 2\theta/l,$$

estimated at large x/l. The values of $R^{\frac{1}{2}}C_D$ thus determined at R = 20–3000 are compared with the results obtained (by numerical solution for the Navier–Stokes equations) by Dennis & Dunwoody (1966) and Dennis & Chang (1969) in table 2. The comparison shows a good agreement.

The broken lines in figure 6 show the displacement thickness. At R = 1200 and 3000, it remains almost constant in the immediate vicinity of the trailing edge, suggesting that it attains a maximum there. At R = 20 the maximum seems to occur in the wake, as in the case of the steady wake of a circular cylinder. Each pair of curves of $R^{\frac{1}{2}}\delta^*/l$ and $R^{\frac{1}{2}}\theta/l$ shows that δ^* approaches the constant value of θ with increasing x/l. This feature can be ascertained from computation using the Gaussian distribution mentioned above.

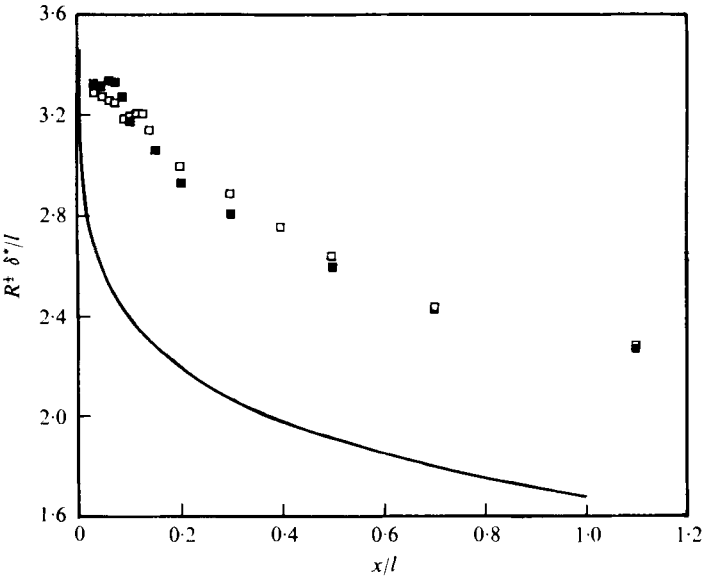

FIGURE 7. Comparison of the non-dimensional displacement thicknesses $R^{\frac{1}{2}}\delta^*/l$ obtained by Goldstein (full line) and in the present experiment (□, $R = 1200$; ■, $R = 3000$).

For the displacement thickness, a comparison is also made in figure 7 between the result of Goldstein (1930, 1933) and the present results for $R = 1200$ and 3000. The theoretical prediction differs from the experimental results in particular immediately behind the trailing edge, as might be supposed from the discussion of figures 1–3.

3.5. *Estimation of streamwise pressure gradient*

We observed that the velocity overshoot appears upstream of the trailing edge and becomes vanishingly small downstream. So we may expect the existence of certain streamwise pressure gradients. Immediately behind the trailing edge, the gradients must be adverse and strongly affect the initial development of the wake. Thus we tried to estimate the pressure gradients within the accuracy of the boundary-layer approximations. Using the approximations, we get the following familiar relation for the gradient in the wake:

$$\frac{1}{1-C_p}\frac{dC_p}{dx} = \frac{2}{2\theta+\delta^*}\frac{d\theta}{dx},$$

where C_p is the pressure coefficient referred to $\frac{1}{2}\rho U_\infty^2$. This states that if $d\theta/dx > 0$ the wake should develop under adverse pressure gradients. This is the case in the near wake, as figure 6 shows. The right-hand side was estimated from the data for δ^* and θ given in figure 6 for the two cases $R = 1200$ and 3000. Thus the average pressure gradients between $x/l = 0{\cdot}0285$ and $0{\cdot}100$ are obtained as

$$\frac{1}{1-C_p}\frac{dC_p}{d(x/l)} = \begin{cases} 0{\cdot}77 \text{ at } R = 1200, \\ 0{\cdot}64 \text{ at } R = 3000. \end{cases}$$

These values are of order unity. The boundary-layer thickness δ_t at the trailing edge is about $0{\cdot}14l$ and $0{\cdot}091l$ at $R = 1200$ and 3000 respectively. So the adverse

pressure gradients exist over a streamwise distance of order δ_t from the trailing edge. Thus, within this distance, Goldstein's prediction under the assumption $dC_p/dx = 0$ in the wake necessarily differs from the present observations, as found in figures 1, 3 and 7. As can be seen from figure 3, the longitudinal diffusion is also large and may not be neglected.

For the reason mentioned above, the flow in the immediate vicinity of the trailing edge should be treated theoretically on the basis of the full Navier–Stokes equations or at least by taking into account the pressure gradient. Such theoretical studies have already been made. For instance, Schneider & Denny (1971) approximately took into account the pressure gradient by applying second-order boundary-layer theory. Using the results to establish the Dirichlet boundary condition over a region enclosing the trailing edge, they also solved the full Navier–Stokes equations. Figure 3 shows that the relation U_c/U_∞ *vs.* x/l obtained from their second-order theory for the flow at $R = 10^5$ comes closer to our experimental data than Goldstein's result. Moreover, in agreement with the present observations, their Navier–Stokes result for the trailing-edge region (up to $x/l = 0{\cdot}001$) shows that U_c/U_∞ varies as $(x/l)^{\frac{1}{2}}$.

4. Conclusion

In this paper we have presented the results of measurements of the velocity distributions in the completely laminar wake behind a finite flat plate at Reynolds numbers of 20–3000. The displacement thickness δ^* and momentum thickness θ were calculated from the experimental velocity distributions, and using the results for $R = 1200$ and 3000, the streamwise pressure gradient in the wake was estimated within the accuracy of the boundary-layer approximations. Goldstein's theoretical results (1930, 1933) for the near and far wake have been compared with the present experimental results in detail.

The following conclusions have been obtained.

(i) At the trailing edge, the experimental velocity distributions for $R = 20$–400 differ from the Blasius distribution appreciably and are accompanied by the characteristic velocity overshoot, whose maximum value is about $0{\cdot}03\,U_\infty$, in the outer part. The distribution approaches the Blasius distribution as the overshoot decreases with increasing Reynolds number.

(ii) In the initial development of the wake, distinct differences appear between the present observations and the theoretical predictions of Goldstein (1930). For instance, the non-dimensional centre-line velocity U_c/U_∞ varies as $(x/l)^{\frac{1}{3}}$ according to his prediction but as $(x/l)^{\frac{1}{2}}$ in the present experiment.

(iii) In the far wake, the velocity distribution U/U_∞ *vs.* $\frac{1}{2}R^{\frac{1}{2}}(y/l)$ is almost independent of R, and Goldstein's (1933) far-wake solution is shown to be in good agreement with the experiment.

(iv) For the wakes at $R = 1200$ and 3000, it is inferred that over a distance of order δ_t from the trailing edge the streamwise pressure gradients are adverse and of order unity.

(v) The drag coefficient estimated from the momentum thickness agrees with the results of Dennis & Dunwoody (1966) and of Dennis & Chang (1969) at each Reynolds number examined.

REFERENCES

DENNIS, S. C. R. & CHANG, G.-Z. 1969 *Phys. Fluids Suppl.* **12**, II 88.
DENNIS, S. C. R. & DUNWOODY, J. 1966 *J. Fluid Mech.* **24**, 577.
GOLDSTEIN, S. 1930 *Proc. Camb. Phil. Soc.* **26**, 1.
GOLDSTEIN, S. 1933 *Proc. Roy. Soc.* A **142**, 545.
GROVE, A. S., PETERSEN, E. E. & ACRIVOS, A. 1964 *Phys. Fluids* **7**, 1017.
HOLLINGDALE, H. S. 1940 *Phil. Mag.* (7), **29**, 209.
MATTINGLY, G. E. & CRIMINALE, W. O. 1972 *J. Fluid Mech.* **51**, 233.
NISHIOKA, M. 1973 *Bull. Japan Soc. Mech. Engrs* **16**, 1887.
NISHIOKA, M. & SATO, H. 1974 *J. Fluid Mech.* **65**, 97.
SATO, H. & KURIKI, K. 1961 *J. Fluid Mech.* **11**, 321.
SCHNEIDER, L. I. & DENNY, V. E. 1971 *A.I.A.A. J.* **9**, 655.
STEWARTSON, K. 1974 *Adv. Appl. Mech.* **14**, 145.
TALKE, F. E. & BERGER, S. A. 1970 *J. Fluid Mech.* **40**, 161.
TANEDA, S. 1956 *J. Phys. Soc. Japan* **11**, 302.